



Article

Asymmetric ferromagnetic criticality in pyrochlore ferromagnet $\text{Lu}_2\text{V}_2\text{O}_7$

Na Su^{a,f,1}, Feiye Li^{b,1}, Yuanyuan Jiao^{a,f,2}, Ziyi Liu^{a,c}, Jianping Sun^{a,f}, Bosen Wang^{a,f,g}, Yu Sui^c, Haidong Zhou^d, Gang Chen^{b,e,*}, Jinguang Cheng^{a,f,g,*}

^aBeijing National Laboratory for Condensed Matter Physics and Institute of Physics, Chinese Academy of Sciences, Beijing 100190, China

^bState Key Laboratory of Surface Physics and Department of Physics, Fudan University, Shanghai 200433, China

^cSchool of Physics, Harbin Institute of Technology, Harbin 150001, China

^dDepartment of Physics and Astronomy, University of Tennessee, Knoxville, TN 37996, USA

^eDepartment of Physics and Center of Theoretical and Computational Physics, The University of Hong Kong, Hong Kong, China

^fSchool of Physical Sciences, University of Chinese Academy of Sciences, Beijing 100190, China

^gSongshan Lake Materials Laboratory, Dongguan 523808, China

ARTICLE INFO

Article history:

Received 20 May 2019

Received in revised form 18 June 2019

Accepted 26 June 2019

Available online 3 July 2019

Keywords:

$\text{Lu}_2\text{V}_2\text{O}_7$ pyrochlore

Ferromagnetic transition

Critical behavior

Ginzburg-Landau analysis

ABSTRACT

We study the ferromagnetic criticality of the pyrochlore magnet $\text{Lu}_2\text{V}_2\text{O}_7$ at the ferromagnetic transition $T_c \approx 70\text{K}$ from the isotherms of magnetization $M(H)$ via an iteration process and the Kouvel-Fisher method. The critical exponents associated with the transition are determined: $\beta = 0.32(1)$, $\gamma = 1.41(1)$, and $\delta = 5.38$. The validity of these critical exponents is further verified by scaling all the $M(H)$ data in the vicinity of T_c onto two universal curves in the plot of $M/|\varepsilon|^\beta$ versus $H/|\varepsilon|^{\beta+\gamma}$, where $\varepsilon = T/T_c - 1$. The obtained β and γ values show asymmetric behaviors on the $T < T_c$ and the $T > T_c$ sides, and are consistent with the predicted values of 3D Ising and cubic universality classes, respectively. This makes $\text{Lu}_2\text{V}_2\text{O}_7$ a rare example in which the critical behaviors associated with a ferromagnetic transition belong to different universality classes. We describe the observed criticality from the Ginzburg-Landau theory with the quartic cubic anisotropy that microscopically originates from the anti-symmetric Dzyaloshinskii-Moriya interaction as revealed by recent magnon thermal Hall effect and theoretical investigations.

© 2019 Science China Press. Published by Elsevier B.V. and Science China Press. All rights reserved.

1. Introduction

As a representative subject of quantum magnetism, pyrochlore antiferromagnets have attracted a significant attention in recent years [1]. Many interesting phenomena including classical spin ice [2,3], quantum spin ice [4–6], pyrochlore ice U(1) spin liquid [5,7–10], quantum order by disorder [11,12], spin nematics [13,14], symmetry enriched topological orders [10,15,16], topological magnetic excitations [17–19] have been proposed and/or discovered for various compounds in the pyrochlore antiferromagnet families. While most efforts of this field have been devoted to the antiferromagnets, the pyrochlore ferromagnet $\text{Lu}_2\text{V}_2\text{O}_7$ may stand out in the field of pyrochlore magnets by providing some rather unique and robust phenomena [20–26].

$\text{Lu}_2\text{V}_2\text{O}_7$ is a vanadium based pyrochlore Mott insulator that orders ferromagnetically below about 70 K. Because the octahedrally coordinated V^{4+} ion has an orbital degree of freedom, the orbitals of the 3d electrons were found to form an ordered pattern, in which each orbital is extended along the local $\langle 111 \rangle$ direction toward the center-of-mass of the V_4 tetrahedron [22,23]. In addition to orbital ordering, this material shows a remarkable magnon thermal Hall transport under magnetic field. Microscopically, the large thermal Hall effect [24,25] in this material is attributed to the non-trivial Berry curvature of the thermally populated magnon bands that originate from the antisymmetric Dzyaloshinskii-Moriya (DM) interaction [24,25,27,28] between the V^{4+} spin-1/2 localized moments on the pyrochlore lattice. Since this discovery, $\text{Lu}_2\text{V}_2\text{O}_7$ has become one of the stereotypes for the thermal Hall transports in Mott insulating materials.

To motivate our work, we here provide a general discussion about the magnetic properties of the pyrochlore ferromagnet $\text{Lu}_2\text{V}_2\text{O}_7$ or any conventionally ordered matter. For the conventional ordered states, there are several basic and phenomenological aspects. The first one would be the order parameter and the ordering structure. Being a ferromagnet is a global static property,

* Corresponding authors.

E-mail addresses: gangchen.physics@gmail.com (G. Chen), jgcheng@iphy.ac.cn (J.G. Cheng).

¹ These authors contributed equally to this work.

² Present address: Faculty of Science, Wuhan University of Science and Technology, Wuhan 430062, China.

$\text{Lu}_2\text{V}_2\text{O}_7$ should have a non-collinear spin structure within the four-sublattice unit cell. This is a direct consequence of the DM interaction. The second one would be the dynamic property or fluctuation with respect to the magnetic order. The thermal Hall transport is an overall effect caused by the magnetic excitations and reflects the weighted average of the Berry curvatures over the magnon bands [24,25]. More detailed information about the dynamics would come from the magnon dispersion directly. This could be obtained through inelastic neutron scattering measurements. Theoretically, it has been suggested that the Weyl magnons [17] may be present from studying a minimal model for $\text{Lu}_2\text{V}_2\text{O}_7$ and can be one origin for the thermal Hall effect in this system [29,30]. The third aspect is the critical property due to the fluctuations of order parameters associated with this ferromagnetic transition in $\text{Lu}_2\text{V}_2\text{O}_7$. This aspect has not been carefully considered. Given the growing interests in this ferromagnetic pyrochlore oxide, we are motivated to explore its critical behaviors around T_C via analyzing the isotherms of magnetization $M(H)$ with an iteration process and the Kouvel-Fisher method. Remarkably, we find that the critical exponents on both sides of T_C are not equal and show 3D Ising-like and 3D cubic-like universality classes on each side. This differs from the conventional wisdom about the criticality that the asymmetry usually occurs in the non-universal prefactors of the scaling law rather than the scaling exponents. We discuss this asymmetric ferromagnetic criticality within Ginzburg-Landau theory and provide our view on the microscopic properties of the V-based pyrochlore magnet $\text{Lu}_2\text{V}_2\text{O}_7$. We further give a general comment about the spin-orbit coupling and the Kitaev physics in the V-based magnets.

The critical behaviors of $\text{Lu}_2\text{V}_2\text{O}_7$ around the ferromagnetic transition can be described by a series of critical exponents β , γ , and δ that reflect the effective magnetic interactions at play [31]. Different critical exponents have been derived theoretically for different models, e.g., $\beta = 0.365$ and $\gamma = 1.386$ for 3D Heisenberg model, $\beta = 0.345$ and $\gamma = 1.316$ for 3D XY model, and $\beta = 0.325$ and $\gamma = 1.24$ for 3D Ising model, respectively [32]. These exponents are obtained by analyzing the isothermal magnetizations $M(H)$ near T_C , viz.

$$M_s(T) \propto (T_C - T)^\beta, \text{ for } T < T_C, \quad (1)$$

$$\chi_0^{-1}(T) \propto (T - T_C)^\gamma, \text{ for } T > T_C, \quad (2)$$

$$M(H) \propto H^{1/\delta}, \text{ for } T = T_C, \quad (3)$$

where M_s is the spontaneous magnetization and χ_0^{-1} is the inverse initial magnetic susceptibility, respectively. In a previous work, Zhou et al. [33] have obtained the critical exponents $\beta = 0.42$ and $\gamma = 1.85$ for $\text{Lu}_2\text{V}_2\text{O}_7$ and ascribed them to a 3D Heisenberg model. However, these values show a large deviation from those predicted theoretically. In addition, the straight lines in the modified Arrott plot, $M^{1/\beta}$ versus $(H/M)^{1/\gamma}$, are not parallel at all. Here, we reinvestigate its critical behaviors around T_C via analyzing the isotherms of magnetization $M(H)$ with an iteration process and the Kouvel-Fisher method. Interestingly, we found that the obtained $\beta = 0.322$ at $T < T_C$ and $\gamma = 1.41$ at $T > T_C$ are close to the predicted values of 3D Ising and 3D Heisenberg or cubic universality classes, respectively.

2. Experimental

$\text{Lu}_2\text{V}_2\text{O}_7$ single crystals used in the present study were grown with the traveling-solvent floating-zone technique. Details about the crystal growth and sample characterizations have been published elsewhere [33]. The magnetic properties of $\text{Lu}_2\text{V}_2\text{O}_7$ were measured with a commercial Magnetic Property Measurement System (MPMS-III, Quantum Design).

3. Results and discussions

In Fig. 1a, we plot the temperature dependence of dc magnetic susceptibility $\chi(T)$ and its inverse $\chi^{-1}(T)$ measured under $\mu_0 H = 0.1$ T in both zero-field-cooled (ZFC) and field-cooled (FC) modes. As can be seen, the ZFC and FC $\chi(T)$ curves are overlapped with each other and the ferromagnetic transition around $T_C \approx 70$ K can be clearly visible from the sharp rise of $\chi(T)$. In the paramagnetic region above T_C , we have applied the Curie-Weiss (CW) fitting to $\chi^{-1}(T)$ in the temperature range 150–300 K and extracted the effective moment of $\mu_{\text{eff}} = 1.89 \mu_B/\text{V}^{4+}$ and the Weiss temperature $\theta_{\text{CW}} = 88.6$ K. The obtained μ_{eff} is closed to expected value of $1.73 \mu_B$ for $S = 1/2$ of V^{4+} , and the deviation from this ideal value originates from the spin-orbit coupling of the V^{4+} ion. The positive θ_{CW} signals the dominant ferromagnetic exchange interactions in this system. Fig. 1b displays the $M(H)$ curve at 2 K, which exhibits a typical ferromagnetic behavior and reaches a saturation moment of $\sim 1.0 \mu_B$ as expected. The coercive field is about 0.003 T as seen from the inset. All these results are consistent with those reported previously and confirm the high quality of the studied crystal [33].

In Fig. 2a, we plot the isothermal $M(H)$ curves of $\text{Lu}_2\text{V}_2\text{O}_7$ in the temperature range of 60–80 K, which covers the ferromagnetic transition. The demagnetization effect has been corrected. Because the studied sample has an irregular shape, we estimated the demagnetization effect from the slope of low-field $M(H_a)$ data, yielding an internal field $H = H_a - DM$ [34]. Since the critical exponents are obtained based on the $M(H)$ data above 1,000 Oe when

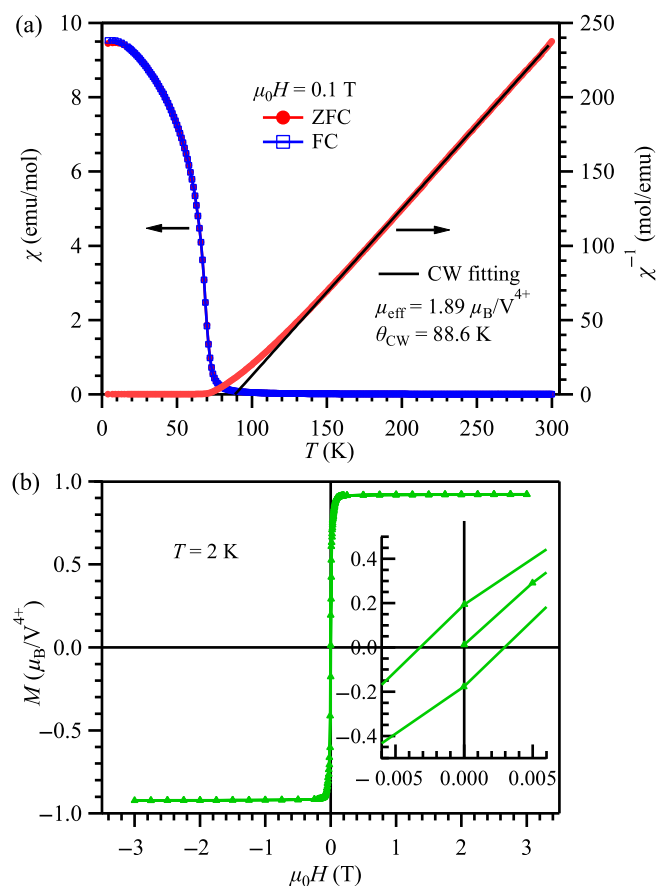


Fig. 1. (Color online) (a) Temperature dependence of dc magnetic susceptibility $\chi(T)$ and its inverse $\chi^{-1}(T)$ measured in both zero-field-cooled (ZFC) and field-cooled (FC) modes under $\mu_0 H = 0.1$ T. The solid line is the Curie-Weiss (CW) fitting curve. (b) Isothermal magnetization $M(H)$ curve at 2 K.

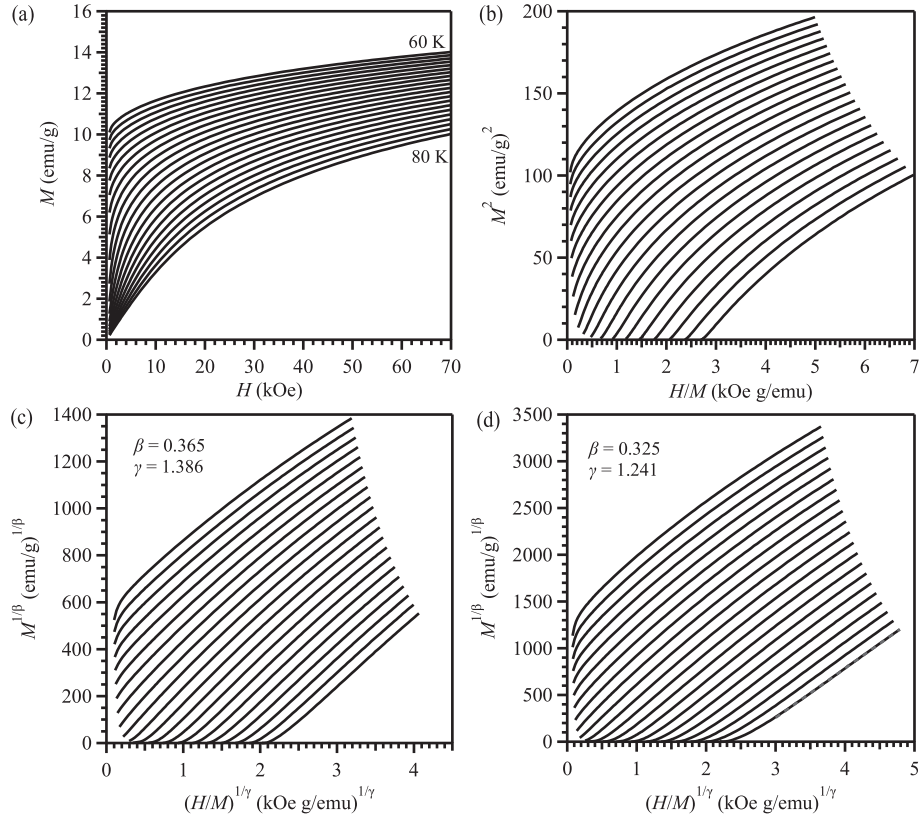


Fig. 2. (a) Isothermal magnetization curves between 60 and 80 K, and the modified Arrott plots of these curves with critical exponents of (b) mean field model $\beta = 0.5$, $\gamma = 1$, (c) 3D Heisenberg model $\beta = 0.365$, $\gamma = 1.386$, and (d) 3D Ising model $\beta = 0.325$, $\gamma = 1.241$.

the $M(H)$ curves tend to saturate, the demagnetization effect has almost no effect on the analysis of the critical behaviors. These $M(H)$ data are replotted in the Arrott plot M^2 vs. H/M in Fig. 2b, and in the modified Arrott plots $M^{1/\beta}$ vs. $(H/M)^{1/\gamma}$ with the critical exponents of 3D Heisenberg and 3D Ising models in Fig. 2c and d, respectively. The curved Arrott plot in Fig. 2b rules out the possibility of mean-field model, but the positive slope of the M^2 vs. H/M confirms that the paramagnet-ferromagnet transition is a continuous transition. On the other hand, the modified Arrott plots in Fig. 2c and d gave roughly parallel straight lines, and it is hard to distinguish visually which model could better describe the ferromagnetism of $\text{Lu}_2\text{V}_2\text{O}_7$.

In order to determine precisely the critical exponents, we employed an iteration process in analyzing the isothermal $M(H)$ data near T_c based on the general formulas (1), (2), (3) given above [35,36]. Starting from the Arrott plot shown in Fig. 2b, we perform third-order polynomial fitting to these M^2 vs. H/M curves and obtain the first set of $M_s(T)$ and $\chi_0^{-1}(T)$ by extrapolating the corresponding fitting curves to the vertical and horizontal axes, respectively. As shown in Fig. 3a, the obtained $M_s(T)$ and $\chi_0^{-1}(T)$ are fitted with the Eqs. (1) and (2), respectively, to extract the first set of critical exponents and critical temperatures, i.e. $\beta = 0.414(6)$, $T_c^- = 71.38(3)$ K, and $\gamma = 1.34(5)$, $T_c^+ = 69.2(3)$ K as listed in the figure. By using the obtained β and γ values, we then construct a modified Arrott plot $M^{1/\beta}$ vs. $(H/M)^{1/\gamma}$ and repeat the above process to obtain the second set of $M_s(T)$ and $\chi_0^{-1}(T)$ and the corresponding critical exponents and critical temperatures. As illustrated in Fig. 3a, after three iterations the fitting parameters are converged to $\beta = 0.322(1)$, $T_c^- = 67.91(1)$ K, and $\gamma = 1.402(3)$, $T_c^+ = 67.7(1)$ K. These critical exponents are different from those reported previously [33].

We further determine the critical exponents by employing the Kouvel-Fisher relation [37], viz.

$$M_s(T)[dM_s/dT]^{-1} = \frac{T - T_c^-}{\beta}, \quad (4)$$

$$\chi_0^{-1}(T)[d\chi_0^{-1}/dT]^{-1} = \frac{T - T_c^+}{\gamma}, \quad (5)$$

in which the $M_s(T)$ and $\chi_0^{-1}(T)$ were obtained from the modified Arrott plot with the final critical exponents obtained above. As shown in Fig. 3b, linear fittings to the plots of $M_s[dM_s/dT]^{-1}$ and $\chi_0^{-1}[d\chi_0^{-1}/dT]^{-1}$ vs. T yield $\beta = 0.322(6)$, $T_c^- = 67.8(1)$ K, and $\gamma = 1.417(4)$, $T_c^+ = 67.7(2)$ K. Both values of β and γ obtained by the Kouvel-Fisher relation agree well with results from the iterations of modified Arrott plot, confirming the validity of these above analysis. For the obtained $\beta = 0.322$ and $\gamma = 1.417$, the modified Arrott plots show nearly perfect parallel straight lines as expected. We then calculated the relative slope $RS = S(T)/S(T_c)$, in which $S(T)$ is the slope of modified Arrott plots at a given temperature T [38]. All the RS values fall into a small range 1 ± 0.08 , thus validating the determined critical exponents β and γ .

For the completeness, we also estimate the critical exponent δ . In Fig. 3c, we display the double logarithmic plot of M vs. H at 68 K, which is very close to the critical temperature $T_c = 67.8(1)$ K determined above. As can be seen, the data fall nearly on a straight line with a slope of $1/\delta$ according to Eq. (3). A linear fitting to the data at high-field region gives $\delta = 5.38$, which fulfills the Widom scaling relation perfectly [39], i.e. $\delta = 1 + \gamma/\beta$ by using $\gamma = 1.417$ and $\beta = 0.322$ obtained above.

To check the reliability of our analysis on the critical behavior of $\text{Lu}_2\text{V}_2\text{O}_7$, we test the obtained critical exponents according to the

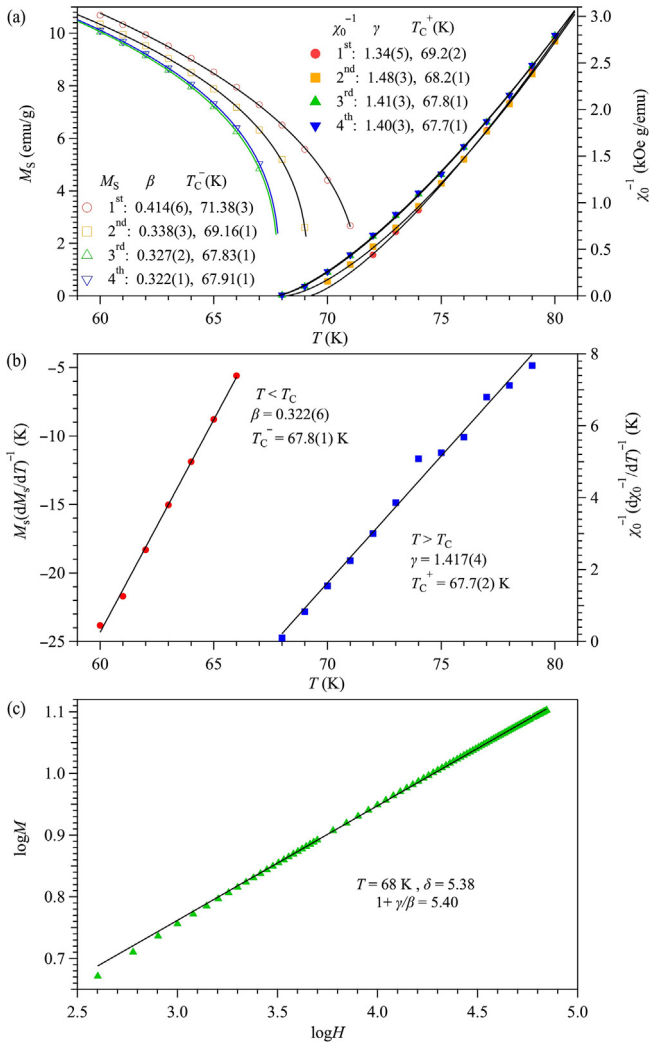


Fig. 3. (Color online) Critical exponents β and γ , and critical temperatures T_C^- and T_C^+ determined from (a) an iteration process started from the mean-field Arrott plot, and (b) Kouvel-Fisher plots. (c) Critical isotherm at $T = 68$ K in a double logarithmic plot and a linear fitting to extract the critical exponent δ . The Widom scaling relation, $\delta = 1 + \gamma/\beta$.

prediction of the scaling hypothesis [31]. In the critical asymptotic region, the magnetic equation of state could be expressed as

$$M(H, \varepsilon) = |\varepsilon|^\beta f_\pm(H/|\varepsilon|^{\beta+\gamma}), \quad (6)$$

where f_+ for $T > T_C$ and f_- for $T < T_C$ are regular analytical functions, and $\varepsilon = T/T_C - 1$ is the reduced temperature. Eq. (6) implies that for the right choice of β , γ , and δ values, $M/|\varepsilon|^\beta$ as a function of $H/|\varepsilon|^{\beta+\gamma}$ should produce two universal curves: one for $T > T_C$ and the other for $T < T_C$. By using the values of β and γ obtained by the Kouvel-Fisher method and $T_C = 67.8$ K, we have obtained the scaling plot shown in Fig. 4. It is clearly seen that all the points indeed collapse into two separate branches. These well-scaled curves in Fig. 4 thus further confirm the reliability of the obtained critical exponents.

We have listed the critical exponents of $\text{Lu}_2\text{V}_2\text{O}_7$ in Table 1 and compared with those of ferromagnetic perovskite YTiO_3 [40] as well as the theoretical values from different models [32,41]. Firstly, we found that the critical exponents for these two ferromagnetic oxides with $S = 1/2$ are stunningly similar with each other. Secondly, it is interesting to note that their β and γ values are not consistent with those predicted by a single model. Instead, β

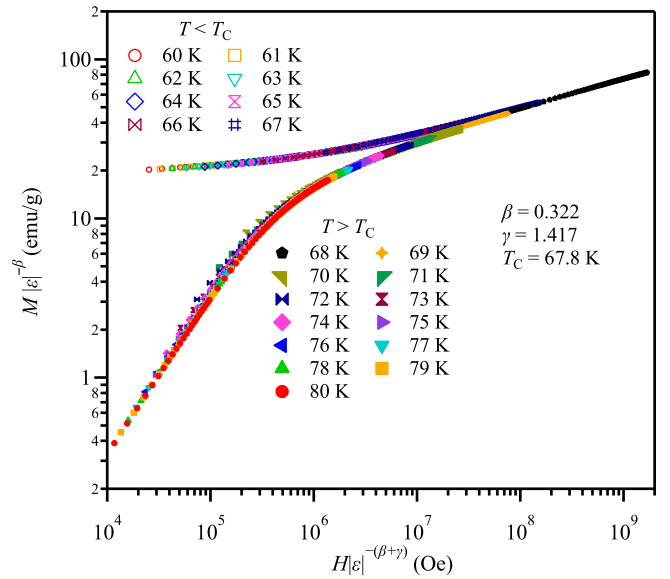


Fig. 4. (Color online) Scaling plot for $\text{Lu}_2\text{V}_2\text{O}_7$ below and above T_C based on the critical temperature $T_C = 67.8$ K and $\beta = 0.322$ and $\gamma = 1.417$.

Table 1

Critical exponents of the single-valent $S = 1/2$ ferromagnetic oxides, $\text{Lu}_2\text{V}_2\text{O}_7$ with the pyrochlore structure and YTiO_3 with the perovskite structure, in comparison with the theoretical values from different models.

	β	γ	δ	Ref.
$\text{Lu}_2\text{V}_2\text{O}_7$	0.322	1.402	5.38	This work
YTiO_3	0.328	1.441	5.39	[40]
3D Ising	0.325	1.241	4.82	[32]
3D XY	0.345	1.316	4.81	[32]
3D Heisenberg	0.365	1.386	4.8	[32]
3D Cubic	0.364	1.390	4.82	[41]

is very close to the predicted value of 3D Ising universality class, whereas γ is close to the predicated value of 3D Heisenberg or cubic universality class. This makes $\text{Lu}_2\text{V}_2\text{O}_7$ and YTiO_3 rather rare cases in which the critical behaviors above and below T_C are described by two different universality classes. This finding is intriguing because the critical behavior associated with a continuous phase transition should be described by one universality class with a single set of critical exponents, and the asymmetric behaviors usually occur in the non-universal prefactors of the scaling relations. The transition from the 3D Heisenberg/cubic to Ising universality class across T_C implies the reduction of spin dimensionality or effective spin components upon the ferromagnetic ordering. As mentioned above, recent experimental and theoretical investigations on $\text{Lu}_2\text{V}_2\text{O}_7$ have revealed the presence of significant anisotropic interactions in the form of DM interaction [24,25,27,28], which should be responsible for such a transition.

It should be noted that the critical exponent δ near T_C is not an independent exponent, but is related with β at $T < T_C$ and γ at $T > T_C$ in terms of $\delta = 1 + \gamma/\beta$ according to the Widom scaling relation. This is indeed confirmed in the present case of $\text{Lu}_2\text{V}_2\text{O}_7$. Since the critical behaviors of ferromagnetic $\text{Lu}_2\text{V}_2\text{O}_7$ undergoes a crossover from 3D Heisenberg at $T > T_C$ to 3D Ising universality class at $T < T_C$, it is naturally expected that the critical exponent δ at T_C should not fulfill any of these universality classes (see Table 1). Whether the observed asymmetric critical behavior in ferromagnetic $\text{Lu}_2\text{V}_2\text{O}_7$ stand for a completely new model deserves further theoretical studies. In addition, to determine the critical exponent α above and below T_C would provide more information about the

asymmetric critical behaviors. We have measured zero-field specific heat of $\text{Lu}_2\text{V}_2\text{O}_7$ crystal near T_c in a very fine step with a commercial Physical Property Measurement System. However, the presence of a round specific-heat anomaly at T_c makes it infeasible for a precise determination of the α exponent in the present case.

The observation of similar critical behaviors in $\text{Lu}_2\text{V}_2\text{O}_7$ and YTiO_3 is not completely unexpected since both V^{4+} and Ti^{3+} ions have identical $3d^1$ electronic configuration with an active orbital degree of freedom in the octahedrally coordinated environments. The active orbitals are the lower t_{2g} orbitals for both compounds. For $\text{Lu}_2\text{V}_2\text{O}_7$, we know that the trigonal distortion would further split the t_{2g} orbitals into a_{1g} orbital and e'_{2g} orbitals. On the other hand, the atomic spin-orbit coupling is active for the t_{2g} orbitals. The spin-1/2 local moment of the V^{4+} ion should be interpreted as the effective spin-1/2 of the ground state Kramers doublet for a local single-ion Hamiltonian with the spin-orbit coupling and the trigonal distortion. From this perspective, the nature of the V^{4+} local moment would be similar to the one for the Ir^{4+} ion, where the latter can be thought as a $5d^1$ hole [42] (instead of $3d^1$ electron for V^{4+}). An interesting consequence of this correspondence is that, the rich physics due to the spin-orbit entanglement for iridates, such as Kitaev interaction [43] and/or highly anisotropic exchange [42], may be found among the 3d transition metal oxides like vanadates.

The orbital nature of the V^{4+} local moment is consistent with the presence of significant (anti-symmetric) DM interaction. Moreover, for the same reason, we expect that the symmetric pseudo-dipolar interaction should be present and equally important as the DM interaction. This may not affect certain topological properties of the magnon bands too much as these properties are topologically robust. Since the local moment is effective spin-1/2, the single-ion anisotropy should not be present. As for the universal long-distance property in the vicinity of the transition, one does not need to worry too much about the detailed form of the interaction. Due to the orbital character of the local moment, the lattice symmetry directly acts on the effective spin components that effectively reduces the ferromagnetic order parameters from having an $O(3)$ symmetry to the cubic symmetry. From the Ginzburg-Landau symmetry analysis, we propose the following action to describe the behavior of $\text{Lu}_2\text{V}_2\text{O}_7$ near the transition,

$$\mathcal{L} = a|\mathbf{M}|^2 + b|\mathbf{M}|^4 + \lambda_c \left[(M^x)^4 + (M^y)^4 + (M^z)^4 \right] + \dots, \quad (7)$$

where \mathbf{M} is the coarse-grained ferromagnetic order parameter, and “...” represents the higher-order terms neglected here. The first two terms are isotropic with $a \approx a'(T - T_c)$, $a' > 0$ and $b > 0$. They can describe the conventional ferromagnetic transition for $O(3)$ -type order parameter, belong to the 3D Heisenberg universality class. We include the cubic anisotropy of the $\text{Lu}_2\text{V}_2\text{O}_7$ system via λ_c and require $\lambda_c < 0$. This cubic anisotropy then favors the order parameter \mathbf{M} to be aligned with the $\langle 001 \rangle$ directions, which is consistent with the experimental observation [24]. For a small λ_c , the system should be found still in the Heisenberg universality class when T is above but not too close to T_c . When T is further tuned to T_c , one expects a crossover from the Heisenberg universality class to the cubic universality class [44]. We mention that the critical exponents belong to these two universality classes are very close, Table 1, thus difficult to be distinguished from each other in experiments. Recent results in literature give $\gamma = 1.3895$ for the Heisenberg class [45] and $\gamma = 1.390$ for the cubic class [41], which are indeed close to the experimental result $\gamma = 1.402$ obtained in this work. At $T < T_c$, the cubic symmetry is spontaneously broken. The system has chosen one of the $\langle 001 \rangle$ directions and the order parameter becomes Ising-like, leading the critical exponent β belong to the Ising universality class. The above Ginzburg-Landau analysis should also apply

to YTiO_3 , but the microscopies are a bit different. Ti^{3+} ion has a cubic lattice geometry and there is no DM interaction on the nearest-neighbor sites.

4. Summary

In summary, we have investigated the critical behavior of ferromagnetic pyrochlore $\text{Lu}_2\text{V}_2\text{O}_7$ based on the measurements of isothermal magnetization $M(H)$ around T_c . We found that the $\beta = 0.322$ at $T < T_c$ and $\gamma = 1.417$ at $T > T_c$ are close to the predicted values of 3D Ising and cubic universality classes, respectively. This makes $\text{Lu}_2\text{V}_2\text{O}_7$ a rare example in which the critical behaviors associated with a ferromagnetic transition belong to different universality classes. We have rationalized the observed criticality from the Ginzburg-Landau theory with the quartic cubic anisotropy that microscopically originates from the anti-symmetric DM interactions.

Conflict of interest

The authors declare that they have no conflict of interest.

Acknowledgments

This work was supported by the National Key R&D Program of China (2018YFA0305700, 2018YFA0305800, 2016YFA0301001 and 2016YFA0300500), the National Natural Science Foundation of China (11574377, 11834016, 11874400), the Strategic Priority Research Program and Key Research Program of Frontier Sciences of the Chinese Academy of Sciences (XDB25000000, XDB07020100 and QYZDB-SSW-SLH013). H. D. Z was supported by NSF DMR 1350002. J.P.S. and Y.Y.J. acknowledge support from the China Postdoctoral Science Foundation and the Postdoctoral Innovative Talent Program.

Author contributions

J.G.C. and G.C. conceived and supervised this project. N.S. and F.Y.L. contributed equally to this work. H.D.Z. prepared the single-crystal sample. N.S., Y.Y.J., Z.Y.L., J.P.S., B.S.W., Y.S., and J.G.C. carried out the magnetic measurements and data analysis. F.Y.L. and G.C. performed theoretical analysis. N.S., F.Y.L., G.C., and J.G.C. wrote the paper. All authors discussed the results and commented on the manuscript.

References

- [1] Gardner JS, Gingras MJP, Greedan JE. Magnetic pyrochlore oxides. *Rev Mod Phys* 2010;82:53–107.
- [2] Castelnovo C, Moessner R, Sondhi SL. Magnetic monopoles in spin ice. *Nature* 2008;451:42–5.
- [3] Bramwell ST, Gingras MJP. Spin ice state in frustrated magnetic pyrochlore materials. *Science* 2001;294:1495–501.
- [4] Molavian HR, Gingras MJP, Canals B. Dynamically induced frustration as a route to a quantum spin ice state in $\text{Tb}_2\text{Ti}_2\text{O}_7$ via virtual crystalfield excitations and quantum many-body effects. *Phys Rev Lett* 2007;98:157204.
- [5] Gingras MJP, McClarty PA. Quantum spinice: a search for gapless quantum spin liquids in pyrochlore magnets. *Rep Prog Phys* 2014;77:056501.
- [6] Ross K, Savary L, Gaulin B, et al. Quantum excitations in quantum spinice. *Phys Rev X* 2011;1:021002.
- [7] Hermele M, Fisher MPA, Balents L. Pyrochlorephotons: the $U(1)$ spin liquid in a $S = \frac{1}{2}$ three-dimensional frustrated magnet. *Phys Rev B* 2004;69:064404.
- [8] Savary L, Balents L. Coulombic quantum liquids in spin-1/2 pyrochlores. *Phys Rev Lett* 2012;108:037202.
- [9] Lee SB, Onoda S, Balents L. Generic quantum spinice. *Phys Rev B* 2012;86:104412.
- [10] Huang YP, Chen G, Hermele M. Quantum spin ices and topological phases from dipolar-octupolar doublets on the pyrochlore lattice. *Phys Rev Lett* 2014;112:167203.
- [11] Savary L, Ross KA, Gaulin BD, et al. Order by quantum disorder in $\text{Er}_2\text{Ti}_2\text{O}_7$. *Phys Rev Lett* 2012;109:167201.

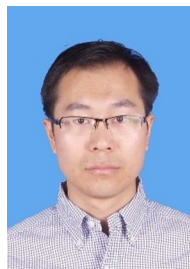
- [12] Hallas AM, Gaudet J, Gaulin BD. Experimental insights into ground-state selection of quantum xyrochlores. *Ann Rev Condensed Matter Phys* 2018;9:105–24.
- [13] Taillefumier M, Benton O, Han LDC, et al. Competing spin liquids and hiddenspin-nematic order in spin ice with frustrated transverse exchange. *Phys Rev X* 2017;7:041057.
- [14] Shannon N, Penc K, Motome Y. Nematic, vector-multipole, and plateau-liquid states in the classical O(3) pyrochlore antiferromagnet with biquadratic interactions in applied magnetic field. *Phys Rev B* 2010;81:184409.
- [15] Chen G. Spectral periodicity of the spinon continuum in quantum spin ice. *Phys Rev B* 2017;96:085136.
- [16] Chen G. Dirac's "magnetic monopoles" in pyrochlore ice u(1) spin liquids: Spectrum and classification. *Phys Rev B* 2017;96:195127.
- [17] Li FY, Li YD, Kim YB, et al. Weyl magnons in breathing pyrochlore antiferromagnets. *Nat Commun* 2016;7:12691.
- [18] Li FY, Chen G. Competing phases and topological excitations of spin-1 pyrochlore antiferromagnets. *Phys Rev B* 2018;98:045109.
- [19] Jian SK, Nie WX. Weylmagnons in pyrochlore antiferromagnets with an all-in-all-out order. *Phys Rev B* 2018;97:115162.
- [20] Bazuev GV, Samokhalov AA, Movozov YN, et al. Magnetic properties of hypovanadates of rare-earth elements having pyrochlorine structure. *Sov Phys Solid State* 1977;19:3274–8.
- [21] Shamoto S, Nakano T, Nozue Y, et al. Substitution effects on ferromagnetic Mott insulator $\text{Lu}_2\text{V}_2\text{O}_7$. *J Phys Chem Solids* 2002;63:1047–50.
- [22] Ichikawa H, Kano L, Saitoh M, et al. Orbital ordering in ferromagnetic $\text{Lu}_2\text{V}_2\text{O}_7$. *J Phys Soc Jpn* 2005;74:1020–5.
- [23] Kiyama T, Shiraoka T, Itoh M, et al. Direct observation of the orbital state in $\text{Lu}_2\text{V}_2\text{O}_7$: a ^{51}V NMR study. *Phys Rev B* 2006;73:184422.
- [24] Onose Y, Ideue T, Katsura H, et al. Observation of the magnon Hall effect. *Science* 2010;329:297–9.
- [25] Ideue T, Onose Y, Katsura H, et al. Effect of lattice geometry on magnon Hall effect in ferromagnetic insulators. *Phys Rev B* 2012;85:134411.
- [26] Choi KY, Wang Z, Lemmens P. Inhomogeneous magnetic cluster states in the magnetoresistance material $\text{Lu}_2\text{V}_2\text{O}_7$. *Phys Rev B* 2010;82:054430.
- [27] Mena M, Perry RS, Perring TG, et al. Spin-wave spectrum of the quantum ferromagnet on the pyrochlore lattice $\text{Lu}_2\text{V}_2\text{O}_7$. *Phys Rev Lett* 2014;113:047202.
- [28] Xiang HJ, Kan EJ, Whangbo MH, et al. Single-ion anisotropy, Dzyaloshinskii-Moriya interaction, and negative magnetoresistance of the spin- $\frac{1}{2}$ pyrochlore $\text{R}_2\text{V}_2\text{O}_7$. *Phys Rev B* 2011;83:174402.
- [29] Su Y, Wang XS, Wang XR. Magnonic Weyl semimetal and chiral anomaly in pyrochlore ferromagnets. *Phys Rev B* 2017;95:224403.
- [30] Mook A, Henk J, Mertig I. Tunable magnon weyl points in ferromagnetic pyrochlores. *Phys Rev Lett* 2016;117:157204.
- [31] Stanley HE. Introduction to phase transitions and critical phenomena. Oxford: Oxford University Press; 1971.
- [32] Kaul SN. Static critical phenomena in ferromagnets with quenched disorder. *J Mag Mag Mater* 1985;53:5.
- [33] Zhou HD, Choi ES, Souza JA, et al. Magnetic-polaron-driven magnetoresistance in the pyrochlore $\text{Lu}_2\text{V}_2\text{O}_7$. *Phys Rev B* 2008;77:020411.
- [34] Kim D, Zink BL, Hellman F, et al. Mean-field behavior with gaussian fluctuations at the ferromagnetic phase transition of SrRuO_3 . *Phys Rev B* 2003;67:100406.
- [35] Yang FY, Chien CL, Li XW, et al. Critical behavior of epitaxial half-metallic ferromagnetic CrO_2 films. *Phys Rev B* 2001;63:092403.
- [36] Yanagihara H, Cheong W, Salamon MB, et al. Critical behavior of single-crystal double perovskite $\text{Sr}_2\text{FeMoO}_6$. *Phys Rev B* 2002:092411.
- [37] Kouvel JS, Fisher ME. Detailed magnetic behavior of nickel near its Curie point. *Phys Rev* 1964;136:A1626–32.
- [38] M'nassri R, Chniba-Boudjada N, Cheikhrouhou A. 3D-Ising ferromagnetic characteristics and magnetocaloric study in $\text{Pr}_{0.4}\text{Eu}_{0.2}\text{Sr}_{0.4}\text{MnO}_3$ manganite. *J Alloys Compd* 2015;640:183–92.
- [39] Widom B. Degree of the critical isotherm. *J Chem Phys* 1964;41:1633–4.
- [40] Cheng JG, Sui Y, Zhou JS, et al. Transition from orbital liquid to Jahn-Teller insulator in orthorhombic perovskites RTiO_3 . *Phys Rev Lett* 2008;101:087205.
- [41] Carmona JM, Pelissetto A, Vicari E. N-component Ginzburg-Landau Hamiltonian with cubic anisotropy: a six-loop study. *Phys Rev B* 2000;61:15136–51.
- [42] Chen G, Balents L. Spin-orbit effects in $\text{Na}_4\text{Ir}_3\text{O}_8$: a hyper-kagomelattice antiferromagnet. *Phys Rev B* 2008;78:094403.
- [43] Jackeli G, Khaliullin G. Mott Insulators in the strong spin-orbit coupling limit: from Heisenberg to a quantum compass and Kitaev models. *Phys Rev Lett* 2009;102:017205.
- [44] Aharony A. Critical behavior of anisotropic cubic systems. *Phys Rev B* 1973;8:4270–3.
- [45] Guida R, Zinn-Justin J. Critical exponents of the N-vector model. *J Phys A Math General* 1998;31:8103.



Na Su obtained her B.S. degree from Lanzhou University in 2014, and M.S. degree from the Institute of Physics, Chinese Academy of Sciences (IOP, CAS) in 2017. She then continued to pursue the doctorate degree in IOP, CAS under the supervision of Prof. Jinguang Cheng. Her current research interest focuses on the exploration and regulation of multiferroic materials under high-pressure conditions.



Gang Chen obtained his Ph.D. degree in theoretical physics from University of California Santa Barbara in 2010. He is currently a faculty at the University of Hong Kong and Fudan University. His research focuses on the strongly correlation physics of quantum condensed matter physics.



Jinguang Cheng obtained his Ph.D. degree from the University of Texas at Austin (UTA) in 2010. After four years of postdoctoral research at UTA and University of Tokyo, he joined the Institute of Physics, Chinese Academy of Sciences and now holds the professor position in the Laboratory of Extreme Conditions Physics. His research focuses on the exploration and study of emergent quantum materials and phenomena under high-pressure extreme conditions.